

Research on the Method of Preparing Microcrystalline Cellulose from Fungal Residue Waste and its Characterization Analysis

Tingwei Zhao,^{a,b} Lijun Shen,^{a,b} Jianjun Yang,^{a,b} Zhi Zheng,^{a,b} Bin Ji,^{a,b} Yinan Peng,^{a,b} and Zhiye Wang^{a,b,*}

In order to alleviate environmental pollution and the waste of resources caused by improper disposal of fungal residue, this study used fungal residue waste, which was treated with NaClO alkaline solution and nitric acid ethanol method for rough fiber preparation. The enzymatic hydrolysis of cellulase conditions were optimized using response surface optimization method, and the optimal preparation parameters were: enzyme addition of 5000 U/g, enzymatic hydrolysis temperature of 52 °C, enzymatic hydrolysis time of 2.65 h, and solid-liquid ratio of 1:20. The Fr-MCC purity reached over 97%. The Fr-MCC obtained had an irregular granular or lamellar aggregation morphology, typical I-type cellulose crystal structure and molecular features, good thermal stability, and was similar in properties to commercial MCC. It was judged to be suitable for further processing and manufacturing of biological base materials. This approach was shown to improve the utilization efficiency of cultivation residues, reducing environmental pollution caused by the accumulation of cultivation residues, and providing new methods and ideas for the preparation of MCC and other bio-based materials.

DOI: 10.15376/biores.19.4.7057-7071

Keywords: Fungal residue; Cellulase; Microcrystalline cellulose; Characterization analysis; Recycling

Contact information: a: Institute of Biology, Gansu Academy of Sciences, Lanzhou 730030, Gansu, China; b: Key Laboratory of Microbial Resources Exploitation and Application of Gansu Province, Lanzhou 730030, Gansu, China; *Corresponding author: zhiye_wang@sina.com

INTRODUCTION

China's edible mushroom industry has developed rapidly into one of the largest edible mushroom crops in the world. Edible mushrooms are delicious and nutritious, and the industry, as a typical high-efficiency agriculture, low-carbon agriculture and sustainable agriculture, is a characteristic industry to improve rural economy and increase farmers' income (Li *et al.* 2022). However, along with huge benefits, there are some problems that need to be solved. Edible mushroom cultivation generates a lot of fungal residues and other waste materials, which may cause certain environmental pollution and resource waste problems if not properly handled. Fungal residue is a waste material produced after edible mushroom cultivation, mainly including wood chips, straw, cottonseed hulls, corn cores, field crop straw and wheat bran, *etc.*, which contain rich crude fiber and other nutrients (Díaz *et al.* 2022). Currently, the proportion of utilization of edible mushroom fungal residues in China is low, and most of them are disposed of by burning, throwing them away, and pulverizing and returning them to the field. This has a certain impact on the ecological environment to some extent, and the bacteria that breed will also

affect the safety of humans and livestock (Maciorowski *et al.* 2007). Proper handling and use of fungal residues in a resourceful, high-value, and scientific way is important to protect the ecological environment and improve the recovery and utilization of agricultural waste.

Cellulose is a natural polysaccharide compound that is widely found in the cell walls of plants. As an important renewable resource, it has many unique properties and broad application prospects. Microcrystalline cellulose (MCC) is a cellulose derivative obtained through special processing, with high crystallinity and microscopic particle size characteristics (Haldar and Purkait 2020). Due to its unique physical and chemical properties, it plays an important role in formulation technology, thickeners, fillers, and carriers. In the past few decades, MCC has become a key raw material in many industries, such as pharmaceuticals, food, textiles, and biomaterials (Trache *et al.* 2016). Currently, according to literature reports, various types of MCC have been prepared from biomass such as bamboo, herbal residues, soybean hulls, and sorghum stalks, using methods such as acid hydrolysis, biological conversion, and oxidation-reduction reactions. Chemical methods are simple and cost-effective and are widely used, while biological methods are environmentally friendly, have mild processing conditions, and are free of pollution, making them a hot topic in cellulose utilization research (Debnath *et al.* 2021).

This study used waste mycelium residue as fungal residue and extracted crude cellulose through NaClO alkaline solution and nitric acid ethanol. Enzymatic hydrolysis parameters were optimized using response surface methodology, and fungus residue microcrystalline cellulose (hereinafter referred to as Fr-MCC) was prepared by enzymatic hydrolysis using cellulase. The Fr-MCC was characterized using scanning electron microscopy (SEM), Fourier transform infrared spectroscopy (FTIR), X-ray diffraction (XRD), and thermogravimetric analysis (TGA), providing theoretical basis and technical support for improving the utilization of waste mycelium residue and preparing new biological materials.

EXPERIMENTAL

Materials

The mycelium residue used in this experiment was from Zhuoni County, Ganzi Tibetan Autonomous Prefecture, with a cellulose content of approximately 36.2%, hemicellulose content of approximately 16.4%, and lignin content of approximately 14.0%. Cellulase was purchased from Beijing Hongrun Baoshun Technology Co., Ltd.

Preparation of Fr-MCC and Enzymatic Hydrolysis Optimization

Extraction of crude fiber

As shown in Fig. 1, the fungus residue was crushed to <1 cm pieces, and visible contaminants such as rubble and debris were removed. The samples were washed clean with tap water and then crushed through a 40-mesh sieve after drying. The samples after screening were mixed with 5% sodium hypochlorite solution (pH was adjusted to 11 with sodium hydroxide solution) at a solid-liquid ratio of 1:10, bleached for 40 min at 55 °C, and washed with tap water for 1 to 2 times. The samples after bleaching were added with nitrate-ethanol solution (nitrate: ethanol=1:3) at a solid-liquid ratio of 1:10, treated with water bath at 80 °C for 60min, washed with tap water to neutral, and blown dry to constant weight to obtain crude cellulose.

Single factor test of enzymatic hydrolysis of Fr-MCC by cellulase

The crude fibers obtained in step a were treated with different solid-liquid ratios (1: 10, 15, 20, 25, 30, 40); cellulase addition amount (500, 1000, 2000, 3000, 4000 u/g (sample)); temperature (35, 45, 55, 65 °C); time (0.5, 1.0, 1.5, 2.0, 2.5, 3, 4, 5 h) as variables, fixed other three factors, the samples were prepared and the samples were washed, centrifuged and dried to obtain the Fr-MCC products, and the effects of each single factor on the yield and purity of Fr-MCC were further investigated.

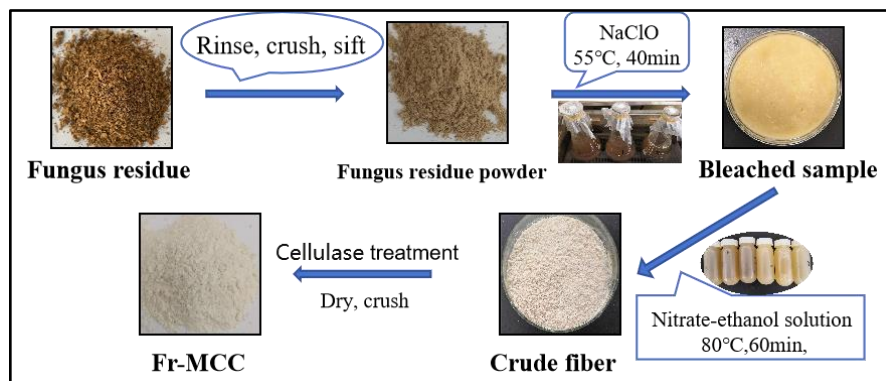


Fig. 1. Preparation flow chart of Fr-MCC

Optimization of preparation parameters by response surface methodology

The purpose of this experiment was to improve the purity of Fr-MCC. On the basis of the above single factor test results, the purity of Fr-MCC was taken as the only response variable, and the enzyme addition, reaction temperature, and reaction time were selected as the three factors for the response surface optimization test of three factors and three levels. The effects of variance analysis and factor interaction on the purity of Fr-MCC were analyzed to optimize the enzymatic hydrolysis preparation parameters.

Determination of Parameters and Analysis Methods

The contents of cellulose, hemicellulose, and lignin in fungal residue raw materials were determined according to Jung *et al.* (2015).

The yield of Fr-MCC was determined according to Ndika *et al.* (2019). The purity was determined according to Ren *et al.* (2018). The Degree of Polymerization (DP) was determined according to Shlieout *et al.* (2002).

The morphology was observed by SEM and compared with references (Sanders 2022). The different test samples, such as Fr-MCC were dispersed in a double-sided conductive adhesive surface and sprayed with gold for 40 seconds at a current of 10 mA. After spraying the gold, the test samples were placed on the sample stage of the scanning electron microscope, and the acceleration voltage was set to 3.0 kV to observe the microscopic morphological features (Kiziltas *et al.* 2014). The Quattro ESEM scanning electron microscope was provided by Thermo Fisher Scientific, Waltham, MA, USA.

For FT-IR analysis (Nicolet Summit X FTIR spectrometer, Thermo Fisher Scientific, Waltham, MA, USA), Fr-MCC and other test sample powders were mixed with an appropriate amount of KBr and then pressed into a sample (Adel *et al.* 2011). Sample were scanned in the range of 400 to 4000 cm^{-1} with a resolution of 4 cm^{-1} .

The XRD analysis used a Cu-K α radiation source with a wavelength of 1.541 Å as the target, 100 mA current, 40 kV acceleration voltage, and 1°/min scanning speed (Ren *et*

al. 2023). The Rigaku X-ray powder diffractometer ULTIMA IV was provided by Japan Physical Science Company. The scanning range of 2θ was 10° to 60° . The relative crystallinity index (CrI) was calculated using the Segal formula,

$$\text{CrI} = (I_{002} - I_{\text{am}}) / I_{002} \quad (1)$$

where I_{002} is the peak intensity of the 002 crystal plane ($2\theta = 22^\circ$), I_{am} is the peak intensity of the amorphous phase, corresponding to $2\theta = 18^\circ$ (Vanhatalo *et al.* 2016).

The TGA analysis was conducted according to the literature reference (Kiziltas *et al.* 2014) using a STA 449 thermogravimetric analyzer (Netzsch, Germany). The sample mass was approximately 6 mg, and the heat stability was determined in an N₂ atmosphere at a flow rate of 40 mL/min from 25 to 900 °C at a heating rate of 10 °C/min.

Statistical Analysis

The data were entered and organized using Microsoft Excel 2010 software, and statistical analysis and graphing were performed using SPSS 17.0 and Origin 2015 software. The analysis of variance between treatments was conducted using the Duncan method at a significance level of 0.05. The response surface optimization was performed using Design-Expert.V8.0.6 software.

RESULTS AND DISCUSSION

Preparation of Fr-MCC by Single-factor Experiment of Enzyme Addition

Effect of enzyme addition on Fr-MCC preparation

The influence of enzyme addition on Fr-MCC yield and purity was studied. As shown in Fig. 2(a), the Fr-MCC yield decreased significantly with the increase of enzyme addition. The purity showed an upward trend, stabilizing at 92.6% when the enzyme addition was 2000 U/ and reaching a maximum of 93.3% at 4000 U/g. The reason for this may be that as the enzyme addition increased, the binding sites between enzyme molecules and cellulose molecules increased, leading to a significant improvement in enzyme decomposition efficiency. The residual hemicellulose, lignin, and amorphous regions adhering to the cellulose surface were mostly decomposed, resulting in an improvement in MCC purity while the yield decreased (Tong *et al.* 2023). In this experiment, the main goal was to improve the purity of Fr-MCC. The optimal range of enzyme addition was selected as 2000 to 5000 U/g for further experiments.

Effect of enzyme hydrolysis temperature on Fr-MCC preparation

The influence of enzyme hydrolysis temperature on Fr-MCC yield and purity was studied. As shown in Fig. 2(b), the Fr-MCC yield showed a downward trend followed by an upward trend with the increase of temperature. There was no significant difference among the treatments within 55 °C, and the yield increased significantly when the temperature exceeded 65 °C, reaching a maximum value of 45.6%. The results of the purity experiment were the opposite, showing an initial increase followed by a sharp decline, reaching a maximum value of 93.5% at 55 °C and a minimum value of 85.0% at 65 °C. This is because the enzymatic reaction activity is easily affected by temperature changes, and when the temperature is low, the enzymatic reaction activity is insufficient, affecting the enzymatic degradation rate of hemicellulose, lignin, *etc.* in the sludge fibers, resulting in low purity and high yield. The Fr-MCC yield and purity underwent significant changed

at 65 °C. This may be due to the fact that the temperature is too high, causing partial inactivation and denaturation of the cellulase, which leads to low purity and high yield (Dalagnol *et al.* 2017). In this experiment, the Fr-MCC purity response surface optimization experiment was conducted in the 45 to 65 °C enzymatic hydrolysis time interval.

Effect of enzymatic hydrolysis time on Fr-MCC preparation

The enzymatic hydrolysis time affected the yield and purity of Fr-MCC. As shown in Fig. 2(c), with the increase of enzymatic hydrolysis time, the Fr-MCC yield decreased significantly, and the decreasing rate accelerated when the time exceeded 2 h. There was no significant change after more than 3 h. The purity results were the opposite of the yield results. When the time exceeded 1.5 h, there was no significant change in purity. The reasons for the decrease in yield and increase in purity may be due to the increase in enzymatic hydrolysis time, which allows the cellulase to react fully, resulting in the degradation of the impurities on the surface of the crude fiber, such as the amorphous region of hemicellulose, into glucose and other monosaccharides and dissolved in water, leading to loss. Until the enzymatic reaction stopped after 3 h, the yield and purity tended to stabilize. In this experiment, the Fr-MCC purity response surface optimization experiment was conducted in the 1 to 3 h interval.

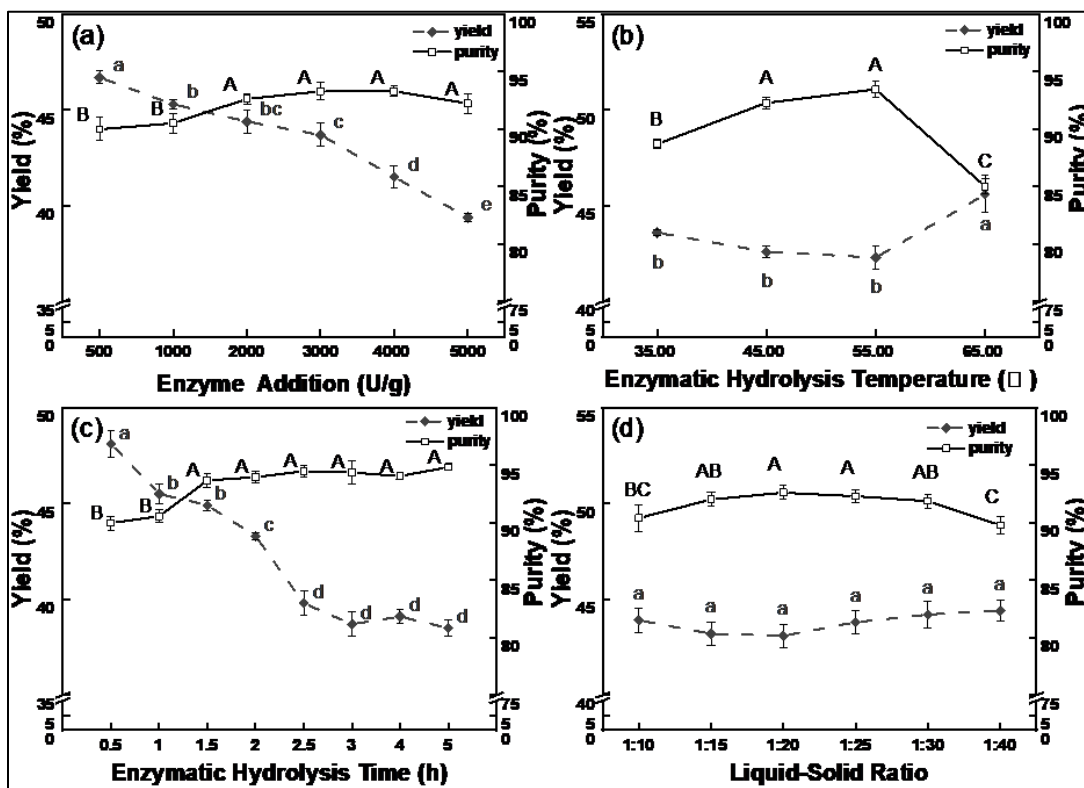


Fig. 2. Effects of cellulase addition (a), temperature (b), time (c), and liquid-solid ratio (d) on the yield and purity of Fr-MCC

Effect of solid-liquid ratio on Fr-MCC preparation

Different solid-liquid ratios of cellulase affected the yield and purity of Fr-MCC. As shown in Fig. 2(d), the yield showed an upward trend within the range of 1:10-40, but it was not significant at any level. The purity showed a trend of first increasing and then decreasing, reaching a maximum value of 92.6% at a solid-liquid ratio of 1:20. The reason for this may be that the liquid volume was too small, and the enzyme solution in the reaction system was not able to completely wrap the reactants, so the enzyme molecules could not fully bind to the cellulose molecules. Alternatively, the liquid volume ratio is too large, causing the enzyme solution concentration to decrease, enzymatic efficiency to decrease, and incomplete enzymatic hydrolysis, resulting in a decrease in the purity of Fr-MCC (Aziz *et al.* 2022). Taking into account the yield, purity, and cost factors, the optimal solid-liquid ratio was judged to be 1:20.

Optimizing the Process Parameters for Fr-MCC Preparation Using Response Surface Methodology

Establishing and analyzing the second-order response surface regression model

Based on the results of the single factor experiment, the Design-Expert.V8.0.6 software was used to conduct a response surface optimization experiment using the Box-Behnken model. Fr-MCC purity was used as the sole response variable, and three variables were selected for analysis: cellulase addition, enzymatic hydrolysis temperature, and enzymatic hydrolysis time. The experimental design and results are shown in Table 1.

Table 1. Experimental Design and Results Based on Response Surface Method

Test No.	Enzyme Addition (U/g)	Temperature (°C)	Time (h)	Purity (%)	
				Predicted value	Actual value
1	2000	45	2	93.63	93.83
2	5000	45	2	93.39	94.41
3	2000	65	2	85.52	87.79
4	5000	65	2	85.43	88.82
5	2000	55	1	92.07	93.46
6	5000	55	1	92.07	94.01
7	2000	55	3	93.10	95.64
8	5000	55	3	93.10	97.97
9	3500	45	1	89.42	91.07
10	3500	65	1	84.77	87.06
11	3500	45	3	92.00	95.71
12	3500	65	3	84.24	88.59
13	3500	55	2	93.51	96.87
14	3500	55	2	93.51	96.72
15	3500	55	2	93.51	96.48
16	3500	55	2	93.51	96.33
17	3500	55	2	93.51	96.13

The variance analysis results are shown in Table 2. The model established through the analysis was significant, and the residual term was not significant, indicating that the model was reasonable. The R^2 value of the model was 0.9971, and the R^2_{adj} value was 0.9934, indicating that the model fit well, and the experimental error was small, which can be used to continue the condition optimization analysis of Fr-MCC purity. Among the coefficients, the main effects of B (enzymatic hydrolysis temperature), C (enzymatic hydrolysis time), and the quadratic term B2 showed a significant impact on purity (P value

< 0.01). The main effects of A (cellulase addition), AC, BC, and the quadratic term C2 had a significant impact on purity (P value < 0.05), and the impact of the three factors on purity in descending order was: enzymatic hydrolysis temperature > enzymatic hydrolysis time > cellulase addition. The fitted second-order polynomial regression equation was as follows:

$$\begin{aligned} \text{Purity} = & -53.24989 + 3.49889 \times 10^{-4} \times A + 5.32055 \times B + 8.45867 \times C \\ & + 7.50000 \times 10^{-6} \times A \times B + 2.96667 \times 10^{-4} \times A \times C - 0.07750 \times B \times C \\ & - 1.40222 \times 10^{-7} \times A^2 - 0.049780 \times B^2 - 0.92050 \times C^2 \end{aligned} \quad (2)$$

Table 2. Variance Analysis of Regression Model for Purity

Variance Source	Square Sum	Degree of Freedom	Mean Square	F-value	P-value	Significance
Model	201.47	9	22.39	268.18	< 0.0001	**
Enzyme addition (A)	2.52	1	2.52	30.19	0.0009	*
Temperature (B)	64.75	1	64.75	775.75	< 0.0001	**
Time (C)	18.94	1	18.94	226.93	< 0.0001	**
AB	0.051	1	0.051	0.61	0.4616	
AC	0.79	1	0.79	9.49	0.0178	*
BC	2.42	1	2.42	28.97	0.0010	*
A ²	0.42	1	0.42	5.02	0.0600	
B ²	104.34	1	104.34	1250.01	< 0.0001	**
C ²	3.57	1	3.57	42.74	0.0003	*
Residue	0.58	7	0.083			
Loss of fit	0.23	3	0.078	0.88	0.5211	
Pure error	0.35	4	0.088			
Sum	202.05	16				

Note: **. Extremely significant difference (P<0.01); *. Significant difference (P<0.05).

Response surface analysis of Fr-MCC purity

By conducting a quadratic regression analysis on the obtained quadratic terms, the interactive effects of AB, AC, and BC can be visualized through a three-dimensional surface plot. The steeper the response surface curve, the more significant the factor's influence on Fr-MCC purity. The bottom projection is an isohyetal map, and the greater the eccentricity, the flatter the shape and the more significant the influence (Li *et al.* 2019). The interactive effects of enzyme addition (A) and enzymatic hydrolysis temperature (B) on Fr-MCC purity are shown in Fig. 3-a, the interactive effects of enzyme addition (A) and enzymatic hydrolysis time (C) on Fr-MCC purity are shown in Fig. 3-b, and the interactive effects of enzymatic hydrolysis temperature (B) and enzymatic hydrolysis time (C) on Fr-MCC purity are shown in Fig. 3-c. From the 3D response surface curve and isohyetal map, the steepness of the surface curve for Fr-MCC purity was in the order of enzymatic hydrolysis temperature being the most significant, followed by enzymatic hydrolysis time, and enzyme addition being the least significant.

Optimal condition prediction and validation experiment

The optimal conditions for enzymatic hydrolysis of xylan to prepare Fr-MCC were predicted and verified through a quadratic regression analysis of the second-order fitting equation. The predicted optimal conditions were approximately: enzyme addition of 5000 U/g, enzymatic hydrolysis temperature of 52 °C, and enzymatic hydrolysis time of 2.65 h. The model predicted that the purity of Fr-MCC could reach up to 98.2%.

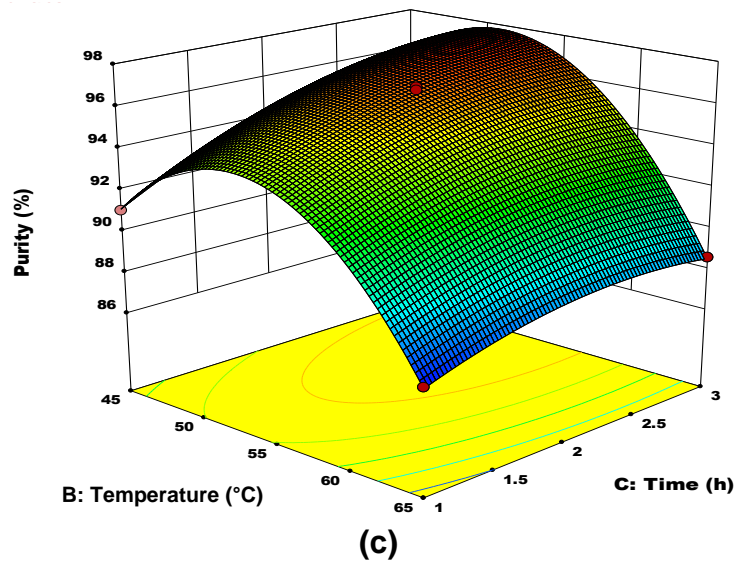
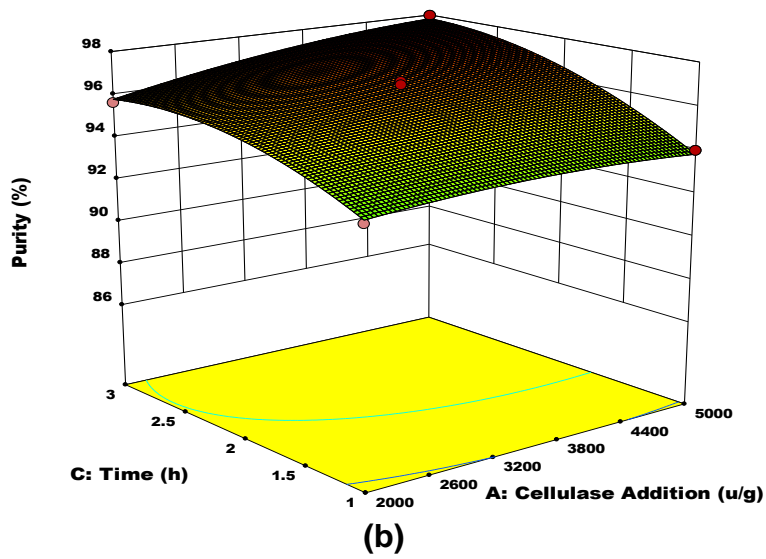
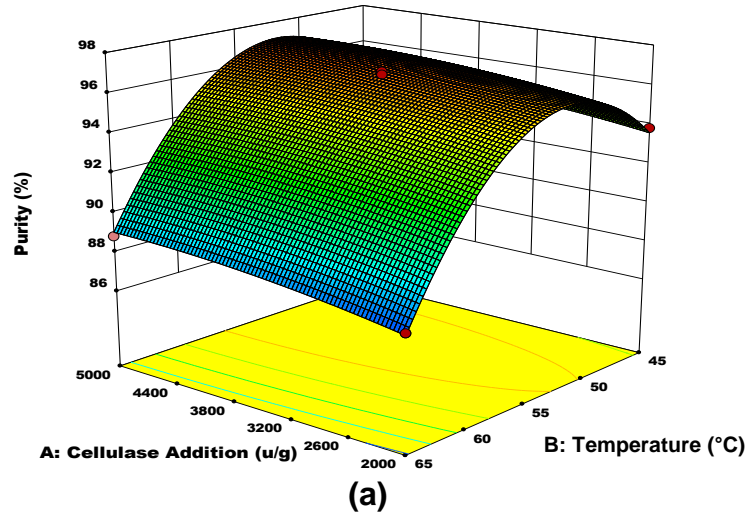


Fig. 3. Effects of interaction for various factors on the purity of Fr-MCC

Five repeated validation experiments were conducted using the predicted optimal conditions, and the actual measured average purity of Fr-MCC was 97.9%, which was only 0.24% lower than the predicted value. This indicates that the model can predict the actual situation fairly well. The degree of polymerization of Fr-MCC was 280.

Structural Characterization Analysis

Scanning electron microscopy (SEM) analysis

The Fr-MCC sample prepared in this experiment was a nearly white powder, with an increased density and more uniform dispersion compared to the fungal residue. Through SEM analysis, the microscopic morphology was observed, as shown in Fig. 4-a. The surface of the fungal residue was relatively smooth and had a high degree of integrity, as the original sample contained lignin, hemicellulose, and cellulose that were adhered together, and were wrapped in wax and protein on the surface (Wang *et al.* 2022). Figure 3-b shows the morphology of the crude fibers after sodium hypochlorite bleaching and nitric acid ethanol treatment. The surface of the crude fibers had a large number of depressions and irregular pores, indicating that the wax layer, protein, and most of the lignin and hemicellulose were decomposed and peeled off, and the internal crystalline structure of cellulose was exposed (Wang *et al.* 2022).

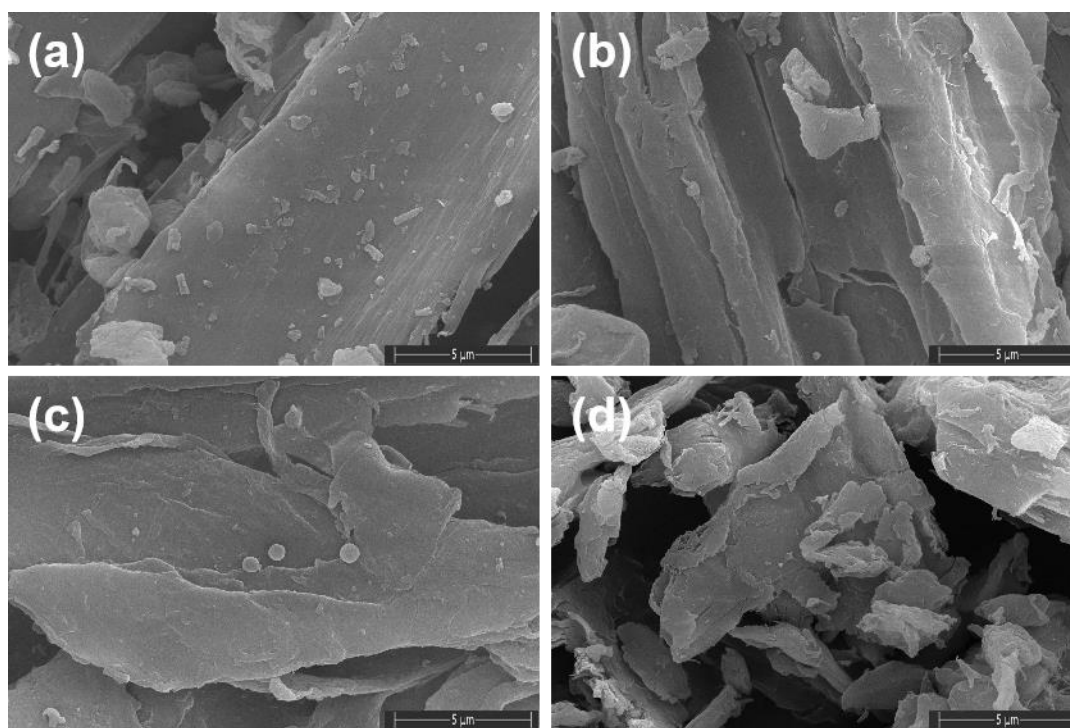


Fig. 4. SEM images for different samples of fungal residue (a), Crude fiber(b), Fr-MCC (c) and Commodity MCC (d)

Figure 3c shows the morphology of Fr-MCC after enzymatic hydrolysis by cellulase, where the sample morphology underwent a noticeable change. Fr-MCC appeared as irregularly shaped, unordered aggregates with a decreased overall particle size and uneven surface texture, indicating that in the presence of cellulase, the long fibers of lignocellulose in the sludge waste were broken down into smaller molecular chains, while lignin and hemicellulose were degraded (Vanitjinda *et al.* 2019). Figure 3d shows the

microscopic morphology of commercial MCC, which has a similar basic shape to Fr-MCC, with irregularly shaped, unordered particles. The main difference is that the commercial MCC particles were smaller, which may be due to the properties of the fungal residue and the degree of comminution.

Fourier transform infrared (FT-IR) analysis

The FT-IR spectra of the fungal residue, crude fiber, Fr-MCC, and commercial MCC are shown in Fig. 5. The peak types of each sample were basically similar, indicating that the functional group structure of cellulose had not changed during the preparation process. The broad absorbance peak at 3336 cm^{-1} was the expression of the stretching of -OH bonds. The absorbance peak height of Fr-MCC during the preparation process showed an upward trend, indicating that the number of free -OH groups had changed. The reason for this may be the enzymatic hydrolysis and breakage of long chain cellulose molecules into short chain cellulose molecules. The absorbance peak at 2892 cm^{-1} was the expression of the stretching vibration of the C-H bonds in methyl, sub-methyl, and next-methyl groups. The peak at 1740 cm^{-1} was attributable to the stretching vibration of lignin, hemicellulose carboxyl ester bond groups, or the stretching vibration of acetyl and xylopyranosyl ester bond groups in hemicellulose. The peak value of Fr-MCC (Fig. 5c) was weakened or disappeared, indicating that the lignin and hemicellulose in it were basically removed. The absorbance peak at 1641 cm^{-1} was ascribed to the variable angle vibration interaction between cellulose and water molecules. The absorbance peak at 1430 cm^{-1} belongs to the bending vibration of the $-\text{CH}_2$ and $-\text{OCH}$ related groups. The weak absorbance peak at 1235 cm^{-1} is the expression of the stretching vibration of the C-O-C ester bond, the fungal residue was much more obvious than the crude fiber, Fr-MCC, and commercial MCC. The absorbance peak at 1164 cm^{-1} represents the stretching vibration of the C-O bond. The absorbance peak at 1029 cm^{-1} represents the skeletal stretching vibration of the C1-O-C4 ring in pyranose sugar. The absorbance peak at 895 cm^{-1} is a structural characteristic peak of cellulose molecules, representing the β -glucosidic bond connection. The increase in the height of the Fr-MCC peak (Fig. 5c) indicates an increase in the purity and crystallinity of cellulose (Kunusa *et al.* 2018).

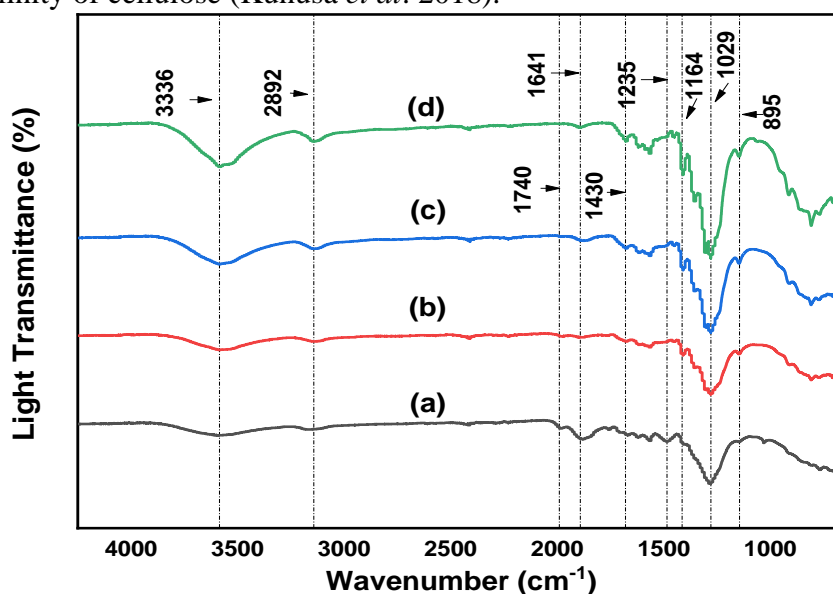


Fig. 5. Comparison of FT-IR spectra for different samples of fungal residue (a), Crude fiber (b), Fr-MCC (c) and commodity MCC (d)

X-ray diffraction (XRD) analysis

The X-ray diffraction pattern is shown in Fig. 6, where all the samples exhibited a strong absorbance peak at $2\theta=22^\circ$, as well as weak peaks at 14° to 17° and 34° , which are all indicative of cellulose I type, suggesting that the cellulose crystal structure was not damaged during the entire preparation process (Naduparambath *et al.* 2018). As shown in Table 3, the crystallinity of several samples was in the order of: commercial MCC > Fr-MCC > rough fibers > raw sample, with crystallinity values of 62.61%, 55.05%, 53.40%, and 38.77%, respectively. This indicates that the crystallinity increased as Fr-MCC was prepared and purified (Murthy *et al.* 1990). The reason for this may be that rough fibers produce H_3O^+ during the acid hydrolysis process, which penetrates the non-crystalline or non-crystalline regions of cellulose molecules, promoting the breakage of sugar glycosidic bonds, ultimately releasing individual microcrystals and resulting in an increase in the crystallinity of rough fibers (Asmarani 2020). Fr-MCC is hydrolyzed by cellulase, where the interwoven lignin and hemicellulose are completely hydrolyzed. This process exposes the internal crystalline state, and in addition, cellulase breaks down the long chain macromolecular cellulose into small molecular cellulose, causing the reorganization of the molecular structure of Fr-MCC, resulting in an increase in its crystallinity (Han and Geng 2023). The high crystallinity of commercial MCC may be due to differences in fungal residue properties and processing methods.

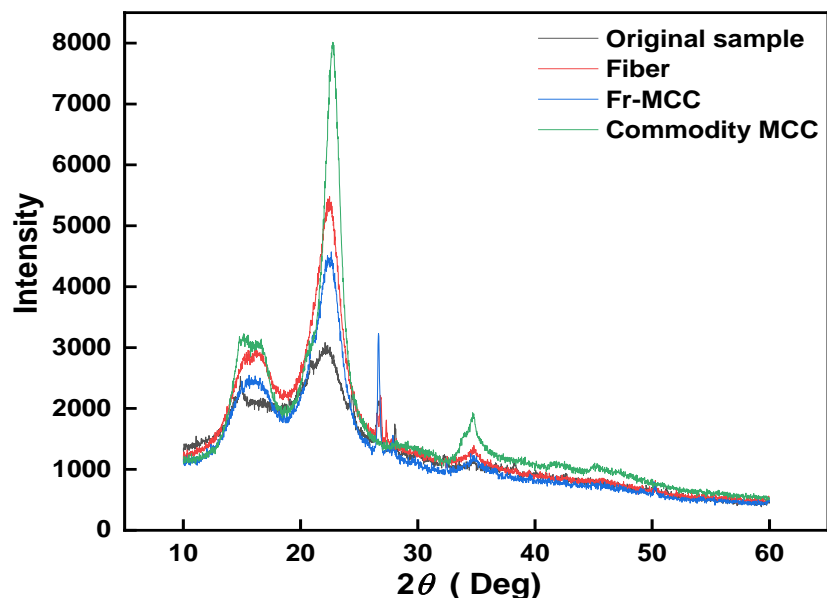


Fig. 6. XRD patterns comparison for different samples of fungal residue, crude fiber, Fr-MCC and Commodity MCC

Table 3. Crystallinity of Fungal Residue, Crude Fiber, Fr-MCC and Commodity MCC

Sample Category	Fungal Residue	Crude Fiber	Fr-MCC	Commodity MCC
CrI/%	38.77	53.40	55.05	62.61

Thermogravimetric analysis (TGA)

As shown in Fig. 7, due to their similar chemical composition, the TG curves of the fungal residue, crude fiber, Fr-MCC, and commercial MCC were basically similar, with the trend of the sample weight loss process being roughly divided into three stages as temperature increases. The first stage occurred at a temperature of approximately 0 to 100 °C, and all four samples showed slight weight loss. This weight loss was caused by the evaporation of free water in the sample (Fielden *et al.* 1988). The weight loss rates are 3.60%, 4.29%, 6.62%, and 4.88%, respectively. The second stage began at approximately 180 and 380 °C for the initial weight loss temperature and maximum weight loss temperature of the fungal residue and crude fiber, respectively, with maximum weight loss percentages of 56.2% and 67.9%, respectively. The initial weight loss temperature of Fr-MCC was 220 °C, the maximum weight loss temperature was 390 °C, and the maximum weight loss was 69.6%. The initial weight loss temperature of commercial MCC was 250 °C, the maximum weight loss temperature was 400 °C, and the maximum weight loss was 82.4%. In the third stage, the TG curves of all four samples became relatively flat, and the weight loss rate stabilized.

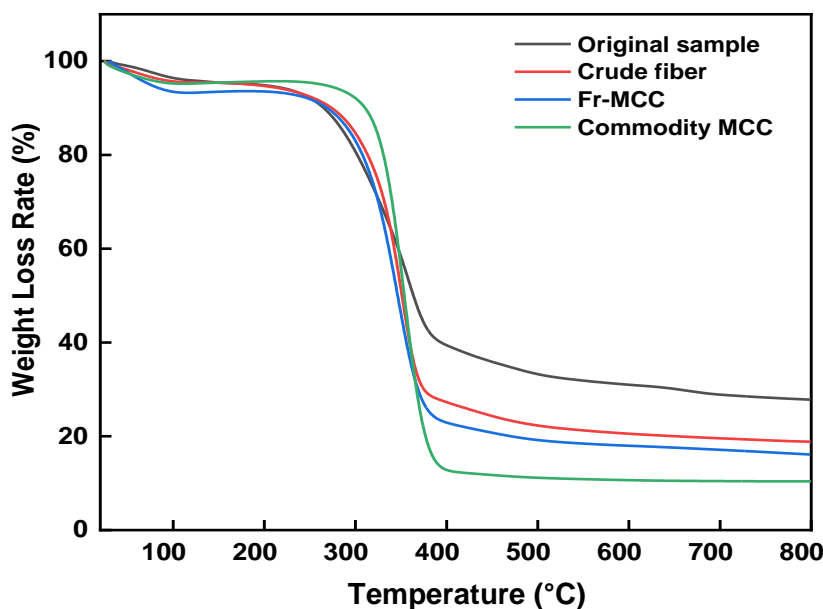


Fig. 7. Comparison of TGA curves for different samples of fungal residue, Crude fiber, Fr-MCC and Commodity MCC

The complete decomposition temperature of the fungal residue, crude fiber, Fr-MCC, and Commercial MCC was 348.5, 342.3, 358.8, and 373.1 °C, respectively, with ash residues of 20.2%, 15.0%, 14.3%, and 5.1%, respectively. Overall, the thermal stability of Fr-MCC was significantly improved compared to the fungal residue and crude fiber samples, but slightly lower than commercial MCC. The thermal stability performance of the four samples is ranked as follows: commercial MCC > Fr-MCC > crude fiber > fungal residue. The reason for this might be that under high-temperature and anaerobic conditions, the biomass undergoes complex processes such as dehydration, depolymerization, isomerization, aromatization, decarboxylation and carbonization, and pyrolysis generates various volatile substances, tar, and residual carbon. This is caused by the fact that the commercial MCC and Fr-MCC have less impurities of all kinds compared to the fungus

residue, and the proportion of residual carbon content is relatively large.

The findings of this study show that there is potential to effectively alleviate the environmental pollution caused by the improper disposal or incineration of fungal residue, and improve the utilization rate of fungal residue waste resources. It provides a new idea and method for the preparation of MCC.

CONCLUSIONS

1. The crude fiber of fungal residue was extracted using NaClO alkaline solution and the nitric acid ethanol method. The optimal enzymatic hydrolysis conditions for preparing high-purity Fr-MCC with cellulase were determined as follows: enzyme addition of 5000 U/g, hydrolysis temperature of 52 °C, hydrolysis time of 2.65 h, and solid-liquid ratio of 1:20, resulting in Fr-MCC purity of over 97%.
2. The sample was in the form of irregular white powder with a crystalline structure, which showed certain thermal stability.

ACKNOWLEDGMENTS

The authors are grateful for the support of the Gansu Provincial Science and Technology Program Youth Science and Technology Fund, Grant No. 23JRRA1665.

REFERENCES CITED

- Adel, A. M., Abd El-Wahab, Z. H., Ibrahim, A. A., and Al-Shemy, M. T. (2011). "Characterization of microcrystalline cellulose prepared from lignocellulosic materials. Part II: Physicochemical properties," *Carbohydrate Polymers* 83(2), 676-687. DOI: 10.1016/j.carbpol.2010.08.039
- Asmarani, G. C. (2020). *Regenerated Amorphous Cellulose from Pineapple Leaf Fibers via Sulfuric Acid Treatment*, Master's Thesis, Chulalongkorn University, Bangkok, Thailand.
- Aziz, T., Farid, A., Haq, F., Kiran, M., Ullah, A., Zhang, K., Li, C., Ghazanfar, S., Sun, H., and Ullah, R. (2022). "A review on the modification of cellulose and its applications," *Polymers* 14(15), 3206. DOI: 10.3390/polym14153206
- Dalagnol, L. M., Silveira, V. C., da Silva, H. B., Manfroí, V., and Rodrigues, R. C. (2017). "Improvement of pectinase, xylanase and cellulase activities by ultrasound: Effects on enzymes and substrates, kinetics and thermodynamic parameters," *Process Biochemistry* 61, 80-87. DOI: 10.1016/j.procbio.2017.06.029
- Debnath, B., Haldar, D., and Purkait, M. K. (2021). "A critical review on the techniques used for the synthesis and applications of crystalline cellulose derived from agricultural wastes and forest residues," *Carbohydrate Polymers* 273, article 118537. DOI: 10.1016/j.carbpol.2021.118537
- Díaz, R., and Díaz-Godínez, G. (2022). "Substrates for mushroom, enzyme and metabolites production: A review," *Journal of Environmental Biology* 43(3), 350-359. DOI: 10.1007/s11274-023-03737-7

- Fielden, K., Newton, J. M., O'Brien, P., and Rowe, R. C. (1988). "Thermal studies on the interaction of water and microcrystalline cellulose," *Journal of Pharmacy and Pharmacology* 40(10), 674-678. DOI: 10.1111/j.2042-7158.1988.tb06993.x
- Haldar, D., and Purkait, M. K. (2020). "Micro and nanocrystalline cellulose derivatives of lignocellulosic biomass: A review on synthesis, applications and advancements," *Carbohydrate Polymers* 250, article 116937. DOI: 10.1016/j.carbpol.2020.116937
- Han, W., and Geng, Y. (2023). "Optimization and characterization of cellulose extraction from olive pomace," *Cellulose* 30(8), 4889-4903. DOI: 10.1007/s10570-023-05195-8
- Jung, S.-J., Kim, S.-H., and Chung, I.-M. (2015). "Comparison of lignin, cellulose, and hemicellulose contents for biofuels utilization among 4 types of lignocellulosic crops," *Biomass and Bioenergy* 83, 322-327. DOI: 10.1016/j.biombioe.2015.10.007
- Kiziltas, A., Gardner, D. J., Han, Y., and Yang, H.-S. (2014). "Mechanical properties of microcrystalline cellulose (MCC) filled engineering thermoplastic composites," *Journal of Polymers and the Environment* 22, 365-372. DOI: 10.1007/s10924-014-0676-5
- Kunusa, W. R., Isa, I., Laliyo, L. A., and Iyabu, H. (2018). "FTIR, XRD, and SEM analysis of microcrystalline cellulose (MCC) fibers from corncobs in alkaline treatment," *Journal of Physics: Conference Series*. DOI: 10.1088/1742-6596/1028/1/012199
- Li, C., and Xu, S. (2022). "Edible mushroom industry in China: Current state and perspectives," *Applied Microbiology and Biotechnology* 106(11), 3949-3955. DOI: 10.1016/j.jclepro.2020.122011
- Li, Y., Li, L., Yasser Farouk, R., and Wang, Y. (2019). "Optimization of polyaluminum chloride-chitosan flocculant for treating pig biogas slurry using the Box-Behnken response surface method," *International Journal of Environmental Research and Public Health* 16(6), article 996. DOI: 10.3390/ijerph16060996
- Maciorowski, K., Herrera, P., Jones, F., Pillai, S., and Ricke, S. (2007). "Effects on poultry and livestock of feed contamination with bacteria and fungi," *Animal Feed Science and Technology* 133(1-2), 109-136.
- Murthy, N., and Minor, H. (1990). "General procedure for evaluating amorphous scattering and crystallinity from X-ray diffraction scans of semicrystalline polymers," *Polymer* 31(6), 996-1002.
- Naduparambath, S., Jinitha, T., Shaniba, V., Sreejith, M., Balan, A. K., and Purushothaman, E. (2018). "Isolation and characterisation of cellulose nanocrystals from sago seed shells," *Carbohydrate Polymers* 180, 13-20. DOI: 10.1016/j.carbpol.2017.09.088
- Ndika, E. V., Chidozie, U. S., and Ikechukwu, U. K. (2019). "Chemical modification of cellulose from palm kernel de-oiled cake to microcrystalline cellulose and its evaluation as a pharmaceutical excipient," *African Journal of Pure and Applied Chemistry* 13(4), 49-57. DOI: 10.5897/AJPAC2019.0787
- Ren, H., Shen, J., Zhu, X., Zhang, B., Fan, W., Wang, Y., and Li, Z. (2018). "Structural characterization and optimization of extraction of microcrystalline cellulose from jerusalem artichoke stalk," *Journal of Chinese Institute of Food Science and Technology* 18(01), 119-127. DOI:10.16429/j.1009-7848.2018.01.016. (in Chinese).
- Ren, H., Xu, Z., Gao, M., Xing, X., Ling, Z., Pan, L., Tian, Y., Zheng, Y., Fan, W., and Yang, W. (2023). "Preparation of microcrystalline cellulose from agricultural residues and their application as polylactic acid/microcrystalline cellulose composite films for the preservation of Lanzhou lily," *International Journal of Biological*

- Macromolecules* 227, 827-838. DOI: 10.1016/j.ijbiomac.2022.12.198
- Sanders, J. E. (2022). *Development and Production of Cellulose Nanocrystal Fillers, PVA Fibers and Composite PVA/CNC Fibers with Electro-Spray/Spinning for Application in Thermoplastic Reinforcement*, Ph.D. Dissertation, The University of Maine, Orono, ME, USA.
- Shlieout, G., Arnold, K., and Müller, G. (2002). "Powder and mechanical properties of microcrystalline cellulose with different degrees of polymerization," *Aaps Pharmscitech* 3, 45-54. DOI: 10.1208/pt030211
- Tong, X., He, Z., Zheng, L., Pande, H., and Ni, Y. (2023). "Enzymatic treatment processes for the production of cellulose nanomaterials: A review," *Carbohydrate Polymers* 299, article 120199. DOI: 10.1016/j.carbpol.2022.120199
- Trache, D., Hussin, M. H., Chuin, C. T. H., Sabar, S., Fazita, M. N., Taiwo, O. F., Hassan, T., and Haafiz, M. M. (2016). "Microcrystalline cellulose: Isolation, characterization and bio-composites application—A review," *International Journal of Biological Macromolecules* 93, 789-804. DOI: 10.1016/j.ijbiomac.2016.09.056
- Vanhatalo, K., Lundin, T., Koskimäki, A., Lillandt, M., and Dahl, O. (2016). "Microcrystalline cellulose property–structure effects in high-pressure fluidization: microfibril characteristics," *Journal of Materials Science* 51, 6019-6034. DOI: 10.1007/s10853-016-9907-6
- Vanitjinda, G., Nimchua, T., and Sukyai, P. (2019). "Effect of xylanase-assisted pretreatment on the properties of cellulose and regenerated cellulose films from sugarcane bagasse," *International Journal of Biological Macromolecules* 122, 503-516. DOI: 10.1016/j.ijbiomac.2018.10.191
- Wang, J., Zhang, R., Quan, C., Shao, X., Hu, N., Yao, X., and Dong, C. (2022). "Green preparation of porous corncob microcrystalline cellulose, and its properties and applications," *Cellulose* 29(13), 7125-7138. DOI: 10.1007/s10570-022-04724-1

Article submitted: May 21, 2024; Peer review completed: July 1, 2024; Revised version received: July 7, 2024; Accepted: July 15, 2024; Published: August 9, 2024.

DOI: 10.15376/biores.19.4.7057-7071